ACS APPLIED MATERIALS & INTERFACES

Research Article

www.acsami.org

Nanoconfinement: an Effective Way to Enhance PVDF Piezoelectric Properties

Valentina Cauda,*[,†,§] Stefano Stassi,[†,‡,§] Katarzyna Bejtka,[†] and Giancarlo Canavese[†,§]

[†]Center for Space Human Robotics@PoliTo, Istituto Italiano di Tecnologia, C.so Trento, 21, 10129 Torino, Italy

[‡]Department of Applied Science and Technology, Politecnico di Torino, C.so Duca degli Abruzzi 24, 10129 Torino, Italy

ABSTRACT: The dimensional confinement and oriented crystallization are both key factors in determining the piezoelectric properties of a polymeric nanostructured material. Here we prepare arrays of one-dimensional polymeric nanowires showing piezoelectric features by template-wetting two distinct polymers into anodic porous alumina (APA) membranes. In particular, poly(vinylidene fluoride), PVDF, and its copolymer poly(vinylidene fluoride-trifluoroethylene), PVTF, are obtained in commercially available APA, showing a final diameter of about 200 nm and several micrometers in length, reflecting the templating matrix features. We show that the crystallization of both polymers into a ferroelectric phase is directed by the nanotemplate confinement. Interestingly, the PVDF nanowires mainly crystallize into the β-phase in the nanoporous matrix, whereas the reference thin film of PVDF crystallizes in the α nonpolar phase. In the case of the PVTF nanowires, needle-like crystals oriented perpendicularly to the APA channel walls are observed, giving insight on the molecular orientation of the polymer within the nanowire structure. A remarkable piezoelectric behavior of both 1-D polymeric nanowires is observed, upon recording ferroelectric polarization, hysteresis, and displacement loops. In particular, an outstanding piezoelectric effect is observed for the PVDF nanowires with respect to the polymeric thin film, considering that no poling was carried out. Current versus voltage (I–V) characteristics showed a consistent switching behavior of the ferroelectric polar domains, thus revealing the importance of the confined and oriented crystallization of the polymer in monodimensional nanoarchitectures.

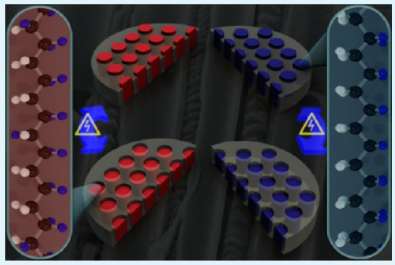

KEYWORDS: *confined PVDF nanowires, nanostructured polymer, template-wetting, piezoelectric properties, anodic porous alumina*

INTRODUCTION

Scaling the size of materials down to the nanometer dimension is offering innovative opportunities not only to study their behavior at the nanoscale but also to discover new useful properties, which can widely extend the range of possible applications.

One of the common strategies to generate monodimensional (1-D) nanostructures is a use of a template filled with the desired material. Several comprehensive reviews on this topic were already published,[1,2] showing that miniaturized, oriented, and anisotropic structures can be prepared by this approach starting from a material precursor or solution. In particular, to form polymeric nanowires, the template-wetting approach from a melt polymer or solution is commonly used.[3] In such a form, the polymer spreads on a porous templating substrate to form a thin surface film, thus covering the pore walls in the initial stages of wetting. Indeed, the polymer preferentially nucleates and grows on the surface of the pore walls, resulting in tubes at short infiltration times. Complete filling of the pores takes place later, and is normally hindered by thermal quenching in the case of melts or by solvent evaporation in the case of solutions; thus, controlled temperature and pressures or a higher amount of feeding material to fill the pores are required.[3,4] The final structure, either a nanotube or a nanowire, shows the same size distribution and shape of the templating matrix. Thus, by appropriately selecting a monodispersed size distribution, as well as aligned and long pores of the templating matrix, one can obtain ordered and monodispersed arrays of nanowires. Several authors have already studied the wetting template in anodic porous alumina (APA) membrane in order to produce arrays of 1-D ceramic and metallic nanowires, showing ferroelectric, dielectric, or conductive properties.[5−7] Porous alumina exhibits a high surface energy, completely wettable by liquids, i.e., polymer melts or solutions.[2] Among several polymers templated into APA,[8,9] the confinement of poly(vinylidene fluoride), PVDF, and its copolymer poly(vinylidene fluoride-trifluoroethylene), PVTF, was reported, obtaining a vertical array of oriented nanowires with a preferential crystalline direction.[10−12] However, despite the nanowire preparation and the study on their crystallization and orientation, to our knowledge, the final piezoelectric properties of these monodimensional polymeric structures were not deeply investigated neither compared to the bulk nor to the thin film form.[13]

Here we report on the preparation of both PVDF and PVTF nanowires into the pores of a templating commercial alumina membrane. This template-directed method is simple, high-throughput, cost-effective, and able to result in nanowires in a single-step procedure. The key point of the present study relies on the preferred crystallization of both polymers into a β

Received: May 9, 2013
Accepted: June 18, 2013
Published: June 18, 2013

   dx.doi.org/10.1021/am4016878 | ACS Appl. Mater. Interfaces 2013, 5, 6430−6437

ferroelectric phase thanks to the nanoconfinement in the alumina channels. We anticipate that the β-phase and the preferential orientation of the crystalline domains lead to a favorable polarization and cause the piezoelectric behavior of the confined nanowires to arise. This behavior is remarkable in the case of PVDF nanowires, because it cannot usually be detected in the thin film without any poling process. In fact, to obtain a measurable piezoelectric answer, the molecules or ferroelectric domains need to be oriented by applying a mechanical stretching or an intense electric field at a certain temperature (poling).[14−17] Other strategies able to achieve the β-phase of the polymorphic PVDF polymer were also previously reported, including the melt,[18,19] using polar solvents,[20] or blending it with small amounts of other polymers.[21,22] These strategies aim to disrupt the strong interchain forces in the α or γ crystalline regions, and use this increased mobility to promote the crystallization into the β-phase. However, they were applied only to bulk and thin films, and in most cases, the piezoelectric properties were not studied.

Here we fully characterize the piezoelectric properties of these polymeric vertical arrays of nanowires, by detecting the piezoelectric displacement, the polarization hysteresis loop, and the current switching peaks by applying an electric field. The aim of this work is to show that a piezoelectric behavior is observed in the absence of any prepoling on the polymeric nanostructures, based on the fact that the nanoconfinement in the alumina pores induces a favorable orientation of the polarization. With this strategy, one can obtain a ready-to-use system, already integrated in a working device or electronic chip, which normally is not able to sustain the high temperatures, intense electric field, or mechanical stresses required for the material poling, as mentioned before.

The advantage of this strategy allows thus the potential preparation of nanosized actuators,[23] ciliated bioinspired sensors,[24] and tactile sensing devices.[25]

EXPERIMENTAL SECTION

Anodic porous alumina membranes (APA, from Anodisc Whatman 47 mm, nominal pore size 200 nm, thickness 60 μm) were cut in four pieces of about 20 × 20 mm^2 and placed on the top of the vacuum sample holder of a spin coater (Spin150 VT BG 66-0, SPS-Europe). Aliquots of 100 μL (2.8 wt %) of poly(vinylidene fluoride) (PVDF, Sigma) in *N*-methyl-pyrrolidone (NMP, Sigma) and of poly(viny fluoride-trifluoro-ethylene) (PVTF, molar ratio PVDF/TrFE = 70/30, Piézotech) in methyl-ethyl ketone (MEK, Sigma) were spin coated for 2 min at 500 rpm and 1 min at 1500 rpm on the APA surface. In order to completely fill the pores of alumina, the wet-impregnation upon spin coating was carried out on both sides of the APA. As a reference, both PVDF and PVTF solutions (10 wt %) in their respective solvents were spin coated (1 min at 3000 rpm) to form thin films of about 1 μm in thickness on conductive platinum coated silicon wafers. All the prepared samples were then treated in the oven at 130 °C for 2 h to improve the crystallization. The templated nanowires into APA membranes were also carefully surface polished, both mechanically and chemically with their respective solvents, in order to remove the polymer excess constituting a film on the membrane surface. Etching of 10 s of the alumina membrane in 4 M NaOH served to improve the access to the top and bottom surfaces of the templated nanowires. To electrically contact the polymeric wires, sputtering of platinum (Pt) electrodes (about 50 nm thick) was carried out on both the top and bottom sides of the polymer-templated APA membranes by means of a Q150TES (Quorum Technology) sputtering system, operating at 50 mA for 180 s at room temperature and 8 × 10^{-4} mbar. Top electrodes were similarly sputtered on the polymeric films deposited on conductive Si wafers.

Field emission scanning electron microscopy (FESEM) characterization was performed with a Dual-Beam Auriga (Carl Zeiss). The cross sections of the samples were prepared with the use of focused ion beam (FIB) in the same instrument. Wide-angle X-ray diffraction patterns were collected on an X'Pert Philips Diffractometer with Cu Kα radiation at λ = 1.5418 Å. Fourier transformed infrared (IR) spectroscopy was carried out in absorption with a Bruker Equinox 55. All spectra were baseline subtracted.

Current−voltage (I−V) curves, ferroelectric polarization hysteresis loops, and piezoelectric displacement measurements were recorded simultaneously by a Piezo Evaluation System (PES, TFAnalyzer 2000HS, Aixacct) coupled to a single point laser vibrometer (Polytec OVF-505), exploiting the converse piezoelectric effect (i.e., generation of a mechanical displacement under the application of an electric field).

RESULTS AND DISCUSSION

Morphological and Structural Characterization. Figures 1 and 2 show the results obtained by template-wetting the APA membranes with both PVTF and PVDF polymers, respectively. The one-step preparation process leads to one-dimensional (1D) nanostructures with a diameter of about 200 nm, thus reflecting the APA template morphology.

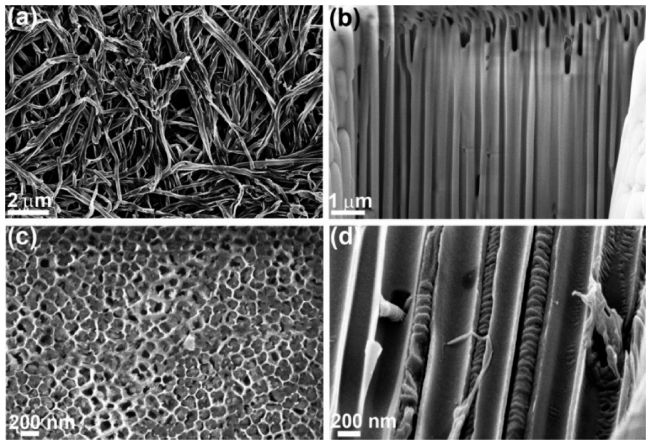

Figure 1. PVTF-templated nanowires in APA: (a) PVTF nanowires after the dissolution of the templating matrix; (b) cross section of the PVTF-templated structures, showing the alumina pore filling; (c) top view of the polymeric-filled APA membrane; (d) magnification of the templated nanowires, showing the crystal orientation in the form of needle-like crystal structures oriented perpendicular to the alumina channel axis.

The polymeric nanowires are several micrometers long, as is also clearly visible upon the template dissolution (Figures 1a and 2a).

The cross section of the membrane reveals a vertically distributed nanowire structure (Figures 1b and 2b) with a good filling ratio (about 80 ± 5%) of the alumina pores by both polymers. However, the top-view image of the filled membrane shows some empty pores (Figures 1c and 2c), indicating that some channels are empty or only partially filled by the polymer (also visible in the cross-section view). This kind of defects will play a role when evaluating the electromechanical properties of the materials as a function of the working electrode area, affecting the piezoelectric and ferroelectric response and enhancing the probability of discharging processes, as discussed later.

Figure 3 shows the FESEM images of the thin films of both PVDF and PVTF. Randomly oriented needle-like crystals are observed on the surface PVTF film (Figure 3a), indicating the semicrystalline structure of the polymeric film. The crystals are approximately 250 nm long and about 50 nm thick. Similar crystalline microdomains closely packed with needle-like shape were also reported in the literature for PVTF.[26] In the case of

dx.doi.org/10.1021/am4016878 | ACS Appl. Mater. Interfaces 2013, 5, 6430−6437

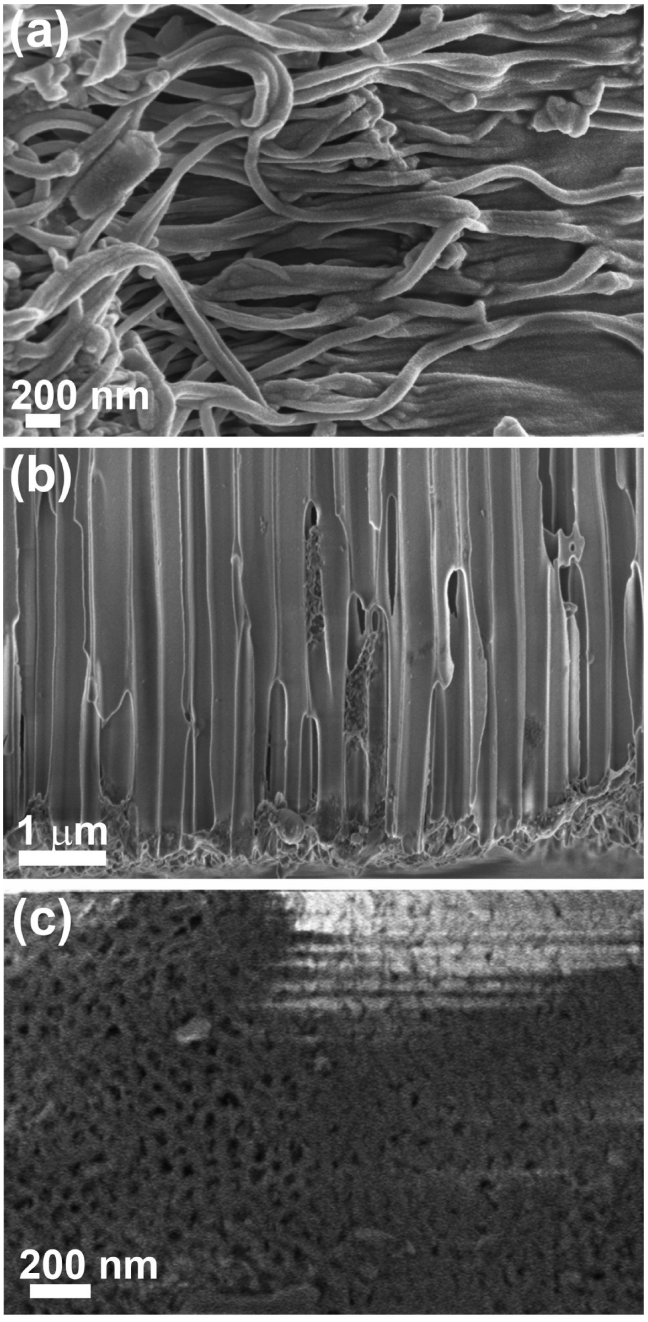

Figure 2. PVDF-templated nanowires in APA: (a) PVDF nanowires obtained upon dissolution of the APA membrane; (b) cross section of the PVDF-templated APA sample, showing the alumina pore filling; (c) top view of the polymeric-filled membrane.

PVDF, smaller and thinner crystals arranged in spherulite-like radial structures are observed (Figure 3b, about 400 nm long and 15 nm thick).

It is worth noting that needle-like crystals were also observed in the PVTF nanowires (Figure 1d), with dimensions close to the alumina channel size, i.e., about 200 nm in length and 20 nm thick. Here the crystals are not randomly oriented as in the PVTF thin film but stacked along the polymeric nanowires and set perpendicularly to the alumina channel axis. This arrangement is attributed to the confinement effect of the alumina pore and confirms what was previously reported in the literature.[10,13,27] Similar crystallites were also investigated in the PVDF wires,

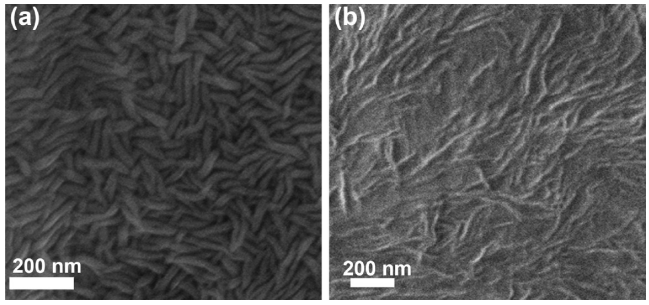

Figure 3. Semicrystalline structure of the polymeric thin films: (a) PVTF; (b) PVDF.

before and after the alumina template dissolution. However, they were not clearly observed in the PVDF nanowires.

The polymer crystallinity in the alumina restricted geometry was studied by X-ray diffraction (Figure 4). The experiment setup was in $\theta-2\theta$ mode, having the scattering vector perpendicular to the alumina membrane surface (as schematically depicted in Figure 4c). Trace A in both diffractograms refers to the empty APA template, only showing a broad bump corresponding to the amorphous alumina. Concerning the PVTF copolymer (Figure 4a), the thin film (trace C) shows the reflections at 19.9°, corresponding to the overlapping of (110) and (200) reflections, at 34.8°, which is the (001), and at 40.7°, due to the overlapping of (111) and (201) reflections, all ascribable to the β ferroelectric phase.[28] The PVTF-templated nanowires (trace B) similarly show the reflection at 19.9°, whereas almost no reflections at 34.8 and 40.7° are observed, confirming the preferential orientation of the β crystals, as observed by FESEM imaging (Figure 1d).

The thin film PVDF reference sample (trace E, Figure 4b) shows several diffraction peaks belonging to the α nonpolar phase at 17.6, 18.4, 20.1, and 27°, corresponding to the (100), (020), and (110) reflections and to the overlapping of (120) and (111) reflections, respectively. Interestingly, the PVDF nanowires templated into APA (trace D) show only a diffraction peak at 19.9° which is tentatively assigned to the β ferroelectric phase, as in the PVTF-related spectra. We attribute this phase change of PVDF to the nanoconfinement into the APA pores. It was previously reported that the β-phase can be induced in the PVDF material by particular treatments.[14,18,19,21,22] However, in the present case, we can exclude any effect of the NMP solvent on the PVDF crystallization in the β-phase, since the diffraction spectra of the PVDF film (prepared under the same conditions) show different reflections, attributed to the α-phase.

IR spectroscopy was carried out on all the nanowire and thin film samples in order to confirm the crystalline phases observed by XRD (Figure 5). The spectrum of the empty template (trace A) is reported for comparison. The polymeric thin film of PVDF from NMP solution (curve E, Figure 5b) shows IR spectra fully ascribable to the α-phase.[29] The α-phase shows an intense absorption band at 763 cm^{-1}, whereas no evidence of the γ-phase (normally observed at both 1233 and 835 cm^{-1}) is found. The PVTF copolymer (trace C) shows a typical spectrum of the β-phase,[29] due to the presence of the peak at 1403, 1280, and 841 cm^{-1}. The band at 1430 cm^{-1} corresponds to the deformation vibration of CH. Both results confirm the previous XRD findings.

In the spectra of the PVTF and PVDF nanowires (curves B and D, respectively), we observed the B1 band at 1403 cm^{-1} corresponding to the β-phase, and related to the wagging vibration of CH_2, having the dipole moment μ_c parallel to the

dx.doi.org/10.1021/am4016878 | ACS Appl. Mater. Interfaces 2013, 5, 6430−6437

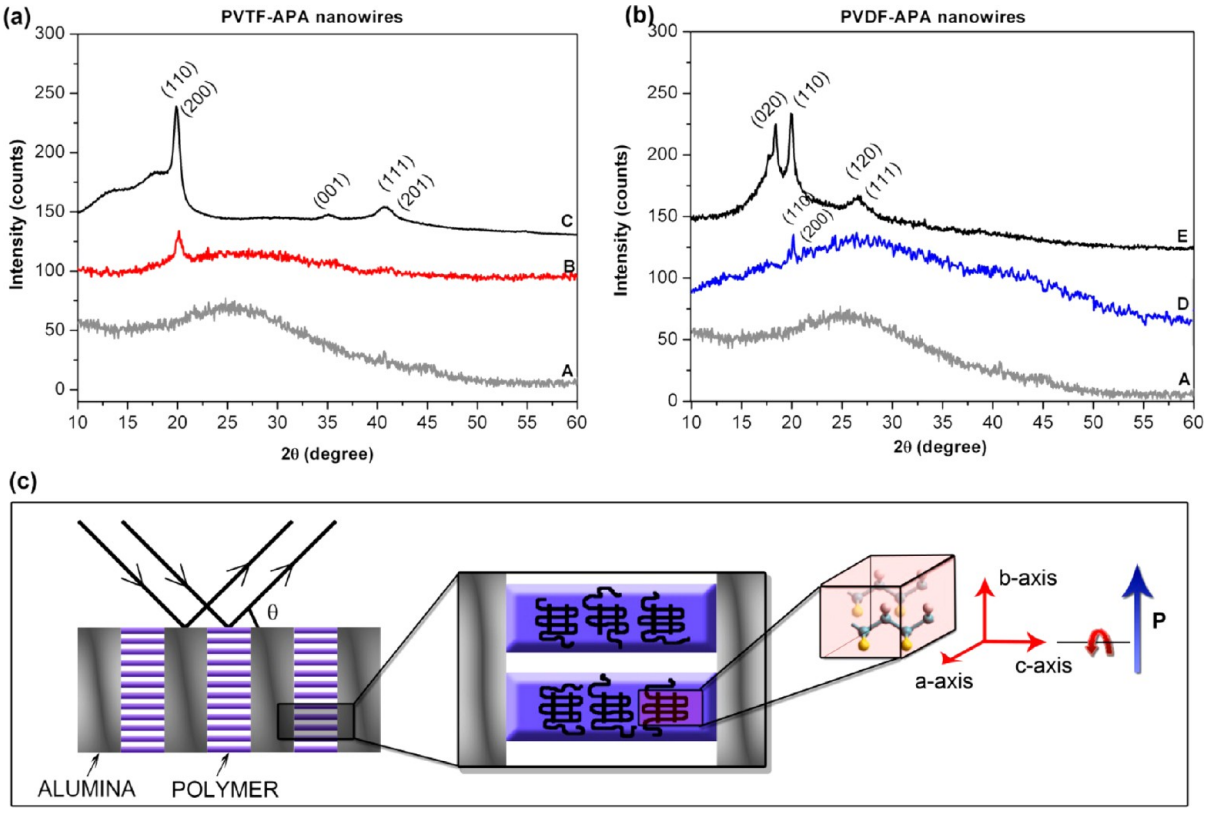

Figure 4. X-ray diffraction (XRD) patterns of the polymeric nanowires templated into APA. (a) PVTF nanowires (trace B in red) are compared to the empty porous alumina (trace A in gray) and the polymer PVTF as a thin film (trace C in black); (b) PVDF nanowires (trace D in blue), compared to the empty APA (trace A in gray) and the PVDF thin film (trace E, in black); (c) schematic representation of the incident X-ray on the polymeric nanowires hosted into the alumina channels (left), showing the orientation of the needle-like crystals of the β-phase (middle). The vertical polar *b*-axis and in-plane *a*- and *c*-axes are also identified (right), leading to a dipole moment (red arrow) turning around the *c*-axis and thus a vertical direction of the polarization *P* (blue arrow).

chain *c*-axis.[30] The presence of this band in the PVDF nanowire spectra confirms thus the XRD findings, ascribing the crystalline diffraction peaks to the β-phase.

Additionally, the bands at 1288 cm^{-1} (A1), observable in the PVTF nanowires, and at 1280 cm^{-1} (A1) for the PVDF nanowires, correspond to the symmetric stretching vibration of CF_2, having a transition dipole moment μ_b parallel to the polar *b*-axis. Other bands at wavenumbers lower than 1200 cm^{-1} are not visible in the polymer-templated samples, due to the huge bump, arising at 1200 cm^{-1}, attributed to the alumina. In summary, high magnification FESEM images and IR and XRD findings show that both the PVTF film and the PVTF−APA nanowires are crystallized in the ferroelectric β-phase. The IR vibration bands and the XRD patterns of the PVDF−AAM nanowires show peaks similar to the PVTF-sample spectra, assigned to the β-phase. In particular, significant differences can be observed among the spectrum of the PVDF−AAM sample and that of PVDF film in both IR and XRD characterizations.

Molecular Orientation. The above results and the literature reports[10,13,30−32] help to understand the molecular orientation of the polymers in the alumina channels. The clearly visible needle-like crystals stacked perpendicularly to the long axis of the PVTF nanowires (Figure 1d) demonstrate that confinement in nanogeometries leads to preferential orientation of semicrystalline polymers. A needle-like crystal is composed of multiple stacks of crystalline lamellae along its axis direction; therefore, the molecular orientation of the polymer chain can be sketched (Figure 4c). The polymeric crystallites grow preferentially flat on the templating surface channel, in order to accommodate the confined environment of the nanotemplate, thus with the *b*-axis parallel to the long axis of the template.[10,31] The *a*- and *c*-axes lie perpendicular to the alumina channel axis. As previously assessed,[31] the *c*-axis should be parallel to the plane of the wall surface of the template, thus facilitating the formation of the nuclei flat on the surface. Due to the circular structure of the templating channels, the labels of both the *a*- and *c*-axes represented in the scheme of Figure 4c are arbitrarily attributed and their position is interchangeable.

Following this molecular scheme, upon the application of a vertical electric field coaxial to the alumina channels, the dipole moment of both polymers should rotate around the *c*-axis, as shown in Figure 4c by the red arrow. Therefore, the polarization *P* (blue arrow) is maximized along the nanowire axis, owing to the vertical orientation of the polar *b*-axis, and results normal to the electrode surface. A good electromechanical coupling can therefore be achieved and the poling of the polymeric nanostructured array is not required to appreciate a piezoelectric behavior, as in contrast usually carried out in the case of bulk or thin films.[14,16,17]

Piezoelectric Functional Characterization. To test the aforementioned hypothesis about the polarization axis orientation, the piezoelectric properties of the template nanowires were characterized by applying an electric field coaxial to the alumina channels and thus to the nanowire axis. To our knowledge, such characterization is applied here for the first time to such confined polymeric nanowires and was reported by some of us for a

dx.doi.org/10.1021/am4016878 | ACS Appl. Mater. Interfaces 2013, 5, 6430−6437

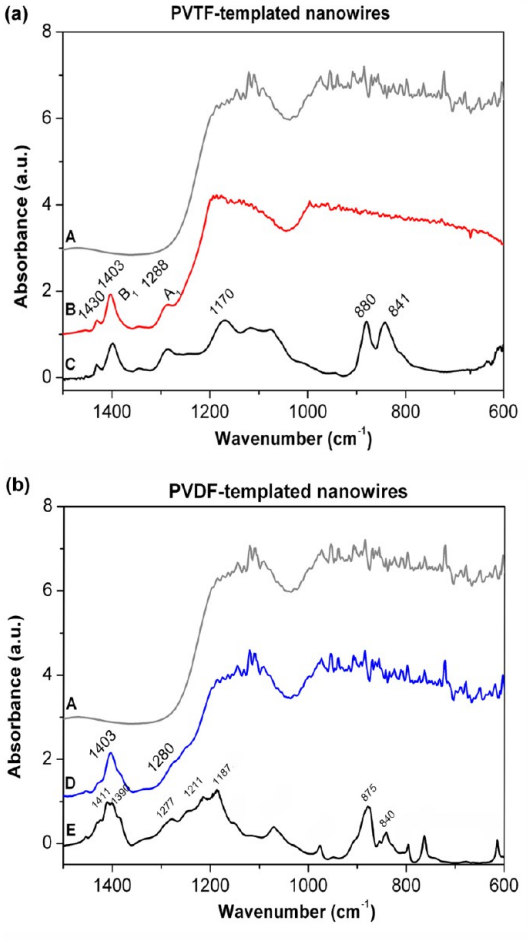

Figure 5. Normalized IR spectra of the polymeric-APA nanowires. (a) PVTF- and (b) PVDF-hosted materials. Trace A, empty APA template; trace B, PVTF nanowires in the APA; trace C, PVTF thin film; trace D, PVDF nanowires in the APA; trace E, PVDF thin film.

different nanostructured system.[13] By applying a triangular voltage stimulus to the polymeric nanowires with the piezo evaluation system, the ferroelectric hysteresis loops, the current switch peaks in the $I-V$ characteristics, and the displacement butterfly loops (Figures 6) were obtained. For the d_{33} hysteresis loop measurements (Figures 7), the small signal technique was employed,[33] by applying a low frequency (0.1 Hz) triangular voltage signal and superimposing a high frequency (2 kHz) sinusoidal signal with an amplitude ~50 times smaller than the triangular one. Both the PVTF- and PVDF-templated nanowires exhibit a ferroelectric behavior, confirmed by the presence of the polarization hysteresis loops and of the current peaks associated with the switching of the polar domains. The shape of the hysteresis curves tends to the rectangular shape of ideal ferroelectric materials but is slightly distorted by the presence of leakage currents in the dielectric, due to defects of the samples (such as empty channels, non-uniform surface, partial filling, etc.).[34] In the case of the PVTF-templated nanowires, the leakage current is very low; thus, it is possible to derive the values of saturation polarization (P_s), remnant polarization (P_r), and coercive field (E_c), neglecting its effect. In contrast, in the PVDF-templated nanowires, the leakage current has a magnitude comparable to the current switching peaks, influencing the shape of the polarization hysteresis loop and masking the ferroelectric properties of the material.

PVTF-templated nanowires show a remnant polarization of 7.4 μC/cm^2 and a saturation polarization of 9.6 μC/cm^2 (Figure 6a), values in line with respect to the as-prepared PVTF thin film (Figure 8a). Further, these measured values are comparable with the literature for both PVDF[35] and PVTF thin films (after a poling step),[36] which are reported in the range 7−15 μC/cm^2. Obviously, our reference thin film of PVDF without any poling step did not show any ferroelectric behavior (data not reported). PVDF-templated nanowires exhibit ferroelectric properties (confirmed by the switching peaks in the current plot of Figure 6b) but show a value of remnant polarization higher than the saturation one (P_r = 19 μC/cm^2 versus P_s = 9 μC/cm^2). This is attributed to the combination of the polarization of the ferroelectric polymer with the charge derived from the superposition of leakage current to the displacement current. Indeed, the leakage current increases the remnant polarization value, since the curves are obtained by an integration of the current response and resulting in a more elliptical shape of the polarization loop (Figure 6b).[34,37]

The nanowires exhibit a very interesting property with respect to the corresponding thin film polymers. For both materials, the coercive field (E_c) is in the range 5−10 V/μm, much lower than 50 V/μm of the bulk samples.[35,38] This effect is associated with the favorable orientation of the polar b-axis of the nanowires, as well as the preferential crystal orientation of the confined polymers into the alumina channels due to the nanometric dimension of the templating matrix. As already observed in other nanometric structures, like a nanocell,[39] the crystal orientation due to the confinement effect leads to a good coupling between the applied electric field and the dipole moment. This property can be very useful for several applications in low-power technology and all-organic electronics,[39] i.e., FeRAM, where easy switchable ferroelectric materials are needed and when only a small electric field can be applied.[35]

The piezoelectric properties of the nanowires are shown in Figures 6c and d and 7 with the displacement butterflies and the d_{33} loops. From the saturation part of the latter plots, d_{33} maximum values of −8.2 and −6.5 pm/V can be extracted for the PVTF- and PVDF-templated nanowires, respectively. For both polymers, the d_{33} value of the nanowires is lower with respect to the film and bulk values. In fact, nonpoled PVTF thin film shows a d_{33} value of about −15 pm/V (Figure 8b), whereas the values reported in the literature for poled film and bulk materials of both PVTF and PVDF are in the range from −20 to −30 pm/V.[36,40] However, no poling process was applied to the templated polymeric nanowires, which is in contrast a fundamental step to obtain any piezoelectric response in PVDF film and bulk samples and to enhance the PVTF piezoelectric properties. Moreover, it should be taken into account that the displacement of the templated nanowires can be reduced by the constriction of the alumina walls. In addition, the working electrode area in contact with the nanowires is quite inferior with respect to the overall Pt-sputtered area, due to the presence of the insulating nonpolar alumina. Indeed, the effective working electrode area should be accounted to 50% of the whole Pt-sputtered area, in reference to the porosity of the alumina membrane. Then, the displacement is attenuated, since it is generated only by the nanowires and not by a uniform surface.

Further improvements of the piezoelectric response, as well as the ferroelectric properties of the templated nanowires, can be obtained by reducing the leakage current, for example, by reducing the defect of the porous templating structure or increasing the filling ratio of the alumina template.

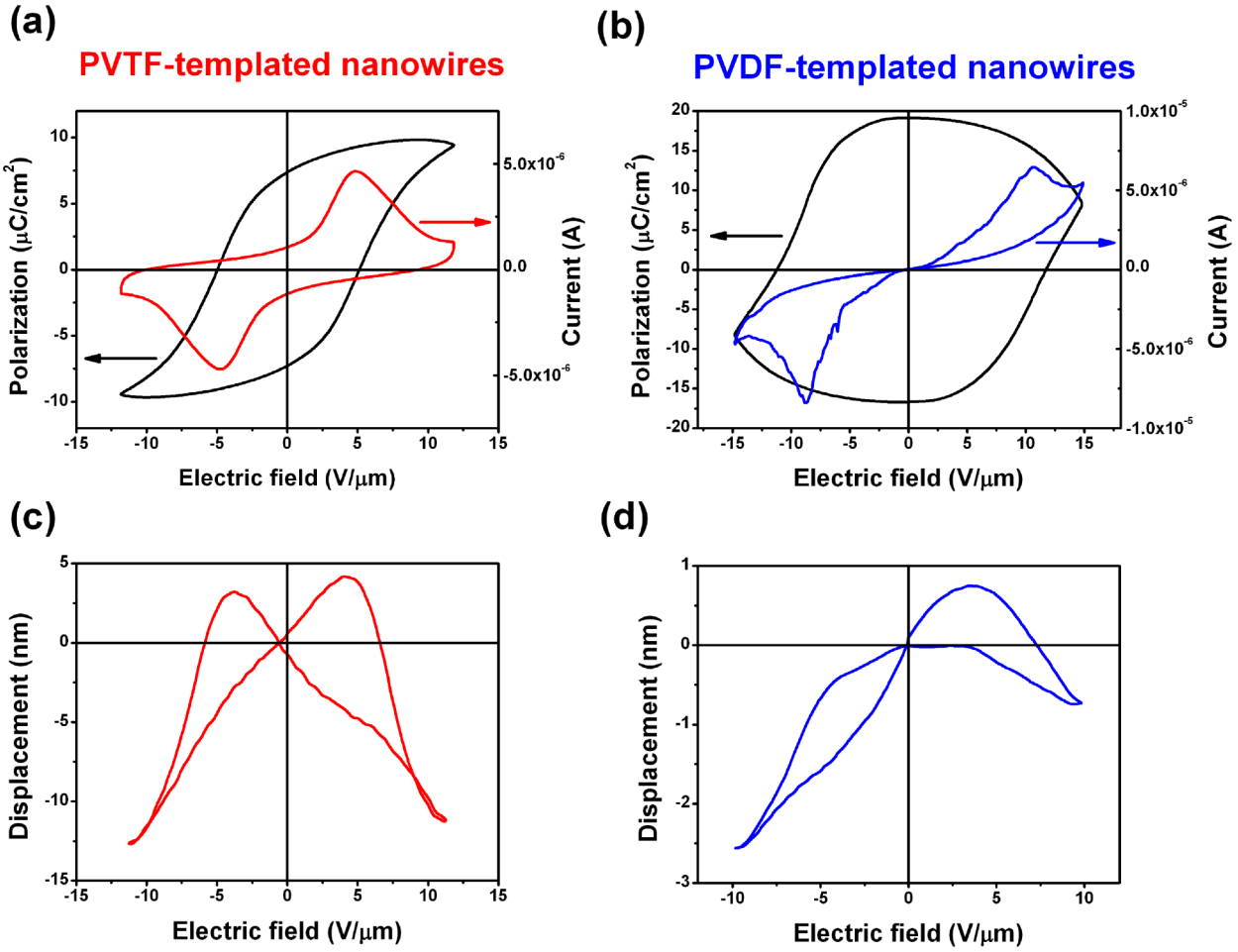

Figure 6. Ferroelectric polarization hysteresis loops, *I*–*V* characteristics, and displacemenent butterflies of (a, c) PVTF- and (b, d) PVDF-templated nanowires in porous alumina.

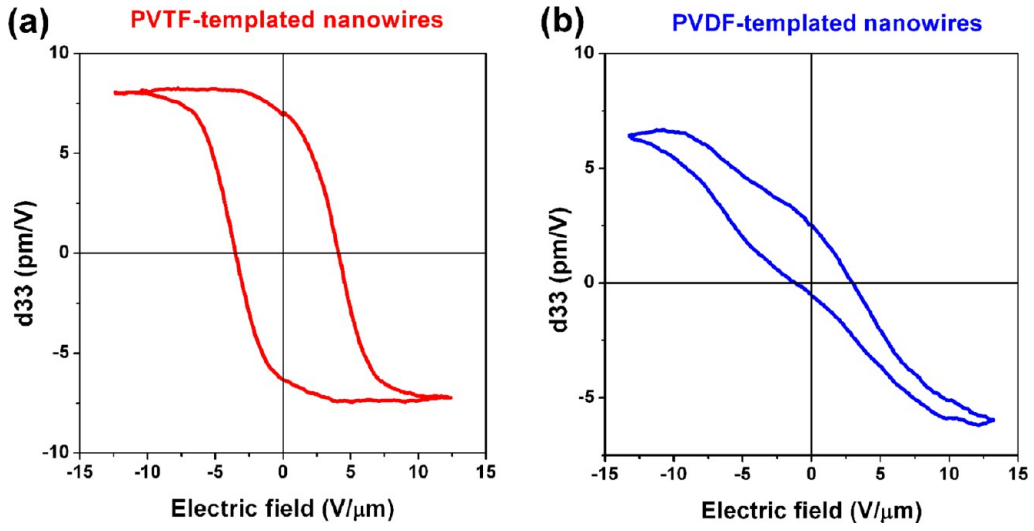

Figure 7. d_{33} curves of (a) PVTF- and (b) PVDF-templated nanowires in porous alumina.

CONCLUSIONS

We have reported on a facile wet-templating method to confine two ferroelectric polymers, PVDF and its copolymer PVTF, into 200 nm sized channels of a commercial 60 μm thick APA. We have shown that the nanoconfinement leads to a preferential crystallization of both polymers in the β ferroelectric phase, showing, in the case of PVTF nanowires, needle-like crystals stacked on top of each other and perpendicular to the APA channel axis. The nanoconfinement induces a change of the crystalline phase of PVDF nanowires from the nonpolar α-phase, present in the polymeric film, to the ferroelectric β one. In addition, a favorable orientation of the polarization axis was

dx.doi.org/10.1021/am4016878 | ACS Appl. Mater. Interfaces 2013, 5, 6430–6437

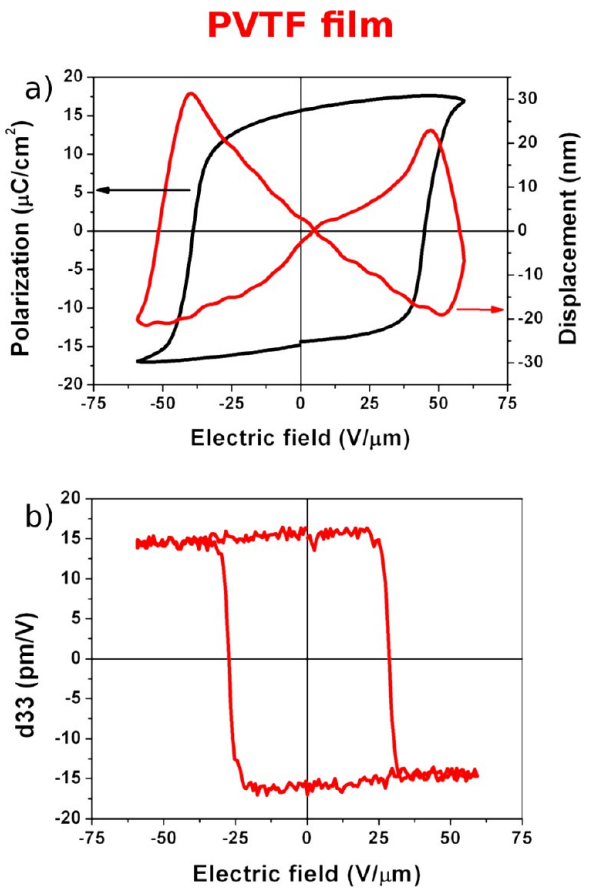

Figure 8. Electromechanical characterization of the PVTF thin film (without poling step): (a) ferroelectric polarization hysteresis loop and displacement butterfly; (b) d_{33} curve of PVTF thin film.

achieved, due to the nanoconfinement. Therefore, by applying an electric field along the polymeric nanowire axis, their electromechanical properties were evaluated, obtaining ferroelectric polarization hysteresis and displacement loops. In particular, a remarkable piezoelectric behavior was observed for the PVDF-templated nanowires, whereas this property is totally absent in the thin film of the same material (without poling). One can than conclude that the nanoconfinement plays a crucial role in the enhancement of the final piezoelectric features of the templated nanowires.

In one preparation step, we can therefore obtain a ready-to-use system showing piezoelectric properties, without any further processing, like electrothermal poling or mechanical stretching.

As a future outlook, these crystalline piezoelectric nanowires distributed in a vertical array into a dielectric membrane can be engineered in piezoelectric micro- or even nanoelectromechanical system devices, thus potentially addressing applications like tactile sensors or nanoactuators.

AUTHOR INFORMATION

Corresponding Author

*Phone: +39 011 090 3436. Fax: +39 011 090 3401. E-mail: valentina.cauda@iit.it.

Author Contributions

§V.C., S.S., G.C.: These authors contributed equally.

Notes

The authors declare no competing financial interest.

ACKNOWLEDGMENTS

The help of Dr. Ilze Aulika for FESEM imaging and FIB processing, Arezio Basteris (Studio Apunto, Torino) for the Table of Contents graphic, and the "Cul de Sac" Team for the fruitful discussion is gratefully acknowledged.

ABBREVIATIONS

APA = anodic porous alumina
PVDF = poly(vinylidene fluoride)
PVTF = poly(vinylidene fluoride-trifluoroethylene)
1-D = monodimensional
FIB = focused ion beam
FESEM = field emission scanning electron microscopy
XRD = X-ray diffraction
IR = infrared spectroscopy
NMP = *N*-methyl-pyrrolidone
MEK = methyl-ethyl ketone
PES = piezo evaluation system

REFERENCES

(1) Xia, Y.; Yang, P.; Sun, Y.; Wu, Y.; Mayers, B.; Gates, B.; Yin, Y.; Kim, F.; Yan, H. *Adv. Mater.* **2003**, *15*, 353−389.
(2) Steinhart, M.; Wendorff, J. H.; Wehrspohn, R. B. *ChemPhysChem* **2003**, *4*, 1171−1176.
(3) Steinhart, M.; Wendorff, J. H.; Greiner, A.; Wehrspohn, R. B.; Nielsch, K.; Schilling, J.; Choi, J.; Gosele, U. *Science* **2002**, *296*, 1997.
(4) Cao, G.; Liu, D. *Adv. Colloid Interface Sci.* **2008**, *136*, 45−64.
(5) Hernandez, B. A.; Chang, K.-S.; Fisher, E. R.; Dorhout, P. K. *Chem. Mater.* **2002**, *14*, 480−482.
(6) Zhang, X. Y.; Zhao, X.; Lai, C. W.; Wang, J.; Tang, X. G.; Daia, J. Y. *Appl. Phys. Lett.* **2004**, *85*, 4190−4192.
(7) Zhao, W.-B.; Zhu, J.-J.; Chen, H.-Y. *J. Cryst. Growth* **2003**, *258*, 176−180.
(8) Zhang, M.; Dobriyal, P.; Chen, J.-T.; Russell, T. P.; Olmo, J.; Merry, A. *Nano Lett.* **2006**, *6*, 1075−1079.
(9) Cepak, V. M.; Martin, C. R. *Chem. Mater.* **1999**, *11*, 1363−1367.
(10) Garcıa-Gutiérrez, M.-C.; Linares, A.; Hernandez, J. J.; Rueda, D. R.; Ezquerra, T. A.; Poza, P.; Davies, R. J. *Nano Lett.* **2010**, *10*, 1472−1476.
(11) Zheng, R. K.; Yang, Y.; Wang, Y.; Wang, J.; Chan, H. L. W.; Choy, C. L.; Jin, C. G.; Li, X. G. *Chem. Commun.* **2005**, 1447−1449.
(12) Cauda, V.; Daprà, D.; Aulika, I.; Chiodoni, A.; Demarchi, D.; Civera, P.; Pizzi, M. *Sens. Transducers J.* **2011**, *12*, 11−17.
(13) Cauda, V.; Torre, B.; Falqui, A.; Canavese, G.; Stassi, S.; Bein, T.; Pizzi, M. *Chem. Mater.* **2012**, *24*, 4215−4221.
(14) Sencadas, V.; Gregorio, R.; Lanceros-Méndez, S. *J. Macromol. Sci., Part B: Phys.* **2009**, *48*, 514−525.
(15) Bai, G.; Li, R.; Liu, Z. G.; Xia, Y. D.; Yin, J. *J. Appl. Phys.* **2012**, *111*, 044102-4−.
(16) Qiu, X. *J. Appl. Phys.* **2010**, *108*, 011101.
(17) Baskaran, S.; He, X.; Wang, Y.; Fu, J. Y. *J. Appl. Phys.* **2012**, *111*, 014109-5−.
(18) Lovinger, A. J. *Polymer* **1981**, *22*, 412−413.
(19) Yang, D.; Chen, Y. *J. Mater. Sci. Lett.* **1987**, *6*, 599−603.
(20) Xu, S.; Wei, Y.; Kirkham, M.; Liu, J.; Mai, W.; Davidovic, D.; Snyder, R. L.; Wang, Z. L. *J. Am. Chem. Soc.* **2008**, *130*, 14958−14959.
(21) Yang, D.; Thomas, E. L. *J. Mater. Sci. Lett.* **1987**, *6*, 593−598.
(22) Rocha, I. S.; Mattoso, L. H. C.; Malmonge, L. F.; Gregório, R. *J. Polym. Sci., Polym. Phys.* **1999**, *37*, 1219−1224.
(23) Berdichevsky, Y.; Lo, Y.-H. *Adv. Mater.* **2006**, *18*, 122−125.
(24) Li, F.; Liu, W.; Stefanini, C.; Fu, X.; Dario, P. *Sensors* **2010**, *10*, 994−1011.
(25) Maheshwari, V.; Saraf, R. *Angew. Chem., Int. Ed.* **2008**, *47*, 7808−7826.
(26) Park, Y. J.; Kang, S. J.; Parkl, C.; Lee, H. S.; Lee, M. S.; Chung, U.-I.; Park, I. J. *Appl. Phys. Lett.* **2006**, *88*, 242908.

(27) Lutkenhaus, J. L.; McEnnis, K.; Serghei, A.; Russell, T. P. *Macromolecules* **2010**, *43*, 3844−3850.
(28) Yoshida, H. *Thermochim. Acta* **1995**, *267*, 239−248.
(29) Benz, M.; Euler, W. B. *J. Appl. Polym. Sci.* **2003**, *89*, 1093−1100.
(30) Hu, Z.; Tian, M.; Nysten, B.; Jonas, A. M. *Nat. Mater.* **2009**, *8*, 62−67.
(31) Hu, Z.; Baralia, G.; Bayot, V.; Gohy, j.-F.; Jonas, A. M. *Nano Lett.* **2005**, *5*, 1738−1743.
(32) Ma, Y.; Hu, W.; Hobbs, J.; Reiter, G. *Soft Matter* **2008**, *4*, 540−543.
(33) Gerber, P.; Kuegeler, C.; Boettger, U.; Waser, R. *J. Appl. Phys.* **2004**, *95*, 4976−4980.
(34) Pintilie, L.; Vrejoiu, I.; Hesse, D.; LeRhun, G.; Alexe, M. *Phys. Rev. B* **2007**, *75*, 224113/1-12.
(35) Heremans, P.; Gelinck, G. H.; Müller, R.; Baeg, K. J.; Kim, D. Y.; Noh, Y. Y. *Chem. Mater.* **2011**, *23*, 341−358.
(36) Omote, K.; Ohigashi, H.; Koga, K. *J. Appl. Phys.* **1997**, *81*, 2760−2769.
(37) Meyer, R.; Waser, R.; Prume, K.; Schmitz, T.; Tiedke, S. *Appl. Phys. Lett.* **2005**, *86*, 1−3.
(38) Naber, R. C. G.; Blom, P. W. M.; Marsman, a. W.; de Leeuw, D. M. *Appl. Phys. Lett.* **2004**, *85*, 2032.
(39) Hu, Z.; Tian, M.; Nysten, B.; Jonas, A. M. *Nat. Mater.* **2009**, *8*, 62−67.
(40) Dargaville, T. R.; Celina, M.; Chaplya, P. M. *J. Polym. Sci., Polym. Phys.* **2005**, *43*, 1310−1320.